

A novel technique to study the fracture of E-glass fiber reinforced composites

G. KISTER, R. BADCOCK, G. F. FERNANDO*

Sensors and Composites Group, Royal Military College of Science, Cranfield University, Shrivenham, Swindon SN6 8LA, UK

E-mail: g.f.fernando@rmcs.cranfield.ac.uk

Conventional techniques for detecting macroscopic damage in fiber-reinforced composites include ultrasonic C-scanning [1, 2], acoustic emission monitoring [3, 4] and thermography [5]. However, these techniques are not capable of imparting information on the fracture sequence of the reinforcing fibers. Information of this nature can be used to validate previous models on the critical number of fibers required to initiate catastrophic failure in fiber-reinforced composites [6, 7]. It can also be used to study the effects of strain transfer from fractured fibers to their immediate neighbors [8, 9]. A detailed study on the conversion of E-glass fibers to act as light guides was reported previously [10]. The waveguides were created by applying an appropriate cladding or coating on the E-glass fiber bundle. A prerequisite here was that the refractive index of the core (E-glass fibers) had to be higher than that of the cladding in order to facilitate total internal reflection of the light in the E-glass fibers. That study also demonstrated that the macroscopic failure of the “mini-composite” could be tracked by monitoring the transmitted light intensity through the fibers as a function of the applied stress. Consequently, the failure of the reinforcing fibers resulted in an attenuation of the transmitted light intensity. In this current study, a CCD-camera was used to image the ends of the E-glass fiber bundle during tensile testing. These images were then used to determine the attenuation of the light intensity and also to obtain information on the fiber fractures over the cross-section of the bundle.

Custom-drawn E-glass fiber bundles were supplied by PPG Industries and these consisted of approximately 2500 individual filaments with an average fiber diameter of 12 μm . The gauge length of the tensile test specimen used was 50 mm and these were end-tapped using Scotch-Weld 9323 adhesive. In order to maintain the light transmission characteristics of the uncoated fibers, a low-refractive index epoxy-based OG135 resin (from Promatech Ltd.) was applied to the fibers that were located within the end-tab region. This was necessary because the refractive index of the end-tab resin was significantly higher than that of the E-glass fibers and hence the conditions for total internal reflection cannot be met. The overall length of the test specimen was 200 mm. A schematic illustration of the test specimen and the associated experimental set-up is illustrated in

Fig. 1. The specimens were tested in tension up to failure at a speed of 0.5 mm/min in an Instron 1195 testing machine under ambient conditions. The applied load was recorded as a function of the time.

With reference to Fig. 1, a 100-mW solid-state green laser (Laser 2000) was used to illuminate one end of the samples and the other end was imaged using a CCD-camera coupled to a 35/210 \times zoom lens (supplied by Cambridge Technology Systems). The light transmission characteristics through the E-glass fiber waveguide was logged by means of a VHS recorder as a function of the time. The light intensity or attenuation of the bundles was evaluated by the difference in the grey levels in the images. The selected bundle-end images were then partitioned into 9 \times 9 arrays to obtain a detailed mapping of the cross-sections. The intensity of the light transmitted through the fibers and the relative spatial distribution across the bundle sections were

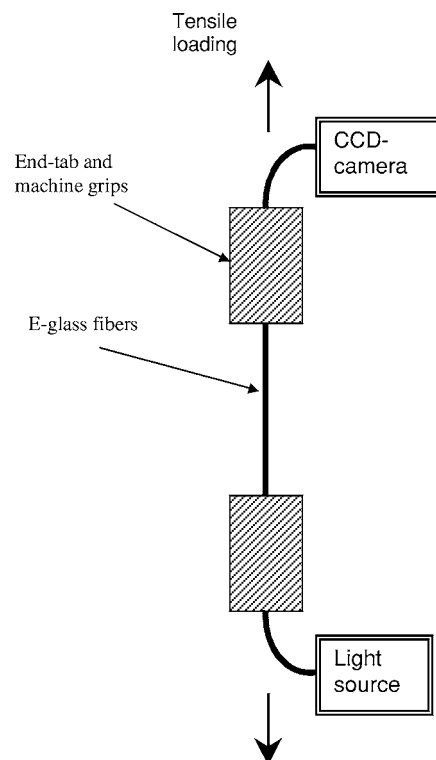


Figure 1 Illustration of the test specimen and the associated experimental set-up.

*Author to whom all correspondence should be addressed.

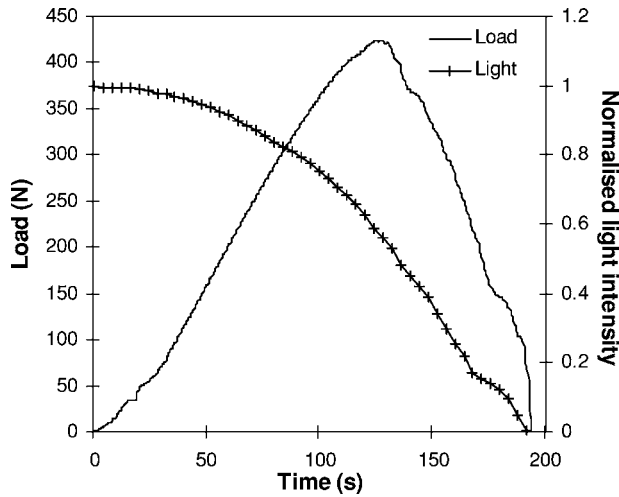


Figure 2 Tensile curve for E-glass fibers and their *in-situ* light transmission variation obtained using a photodiode.

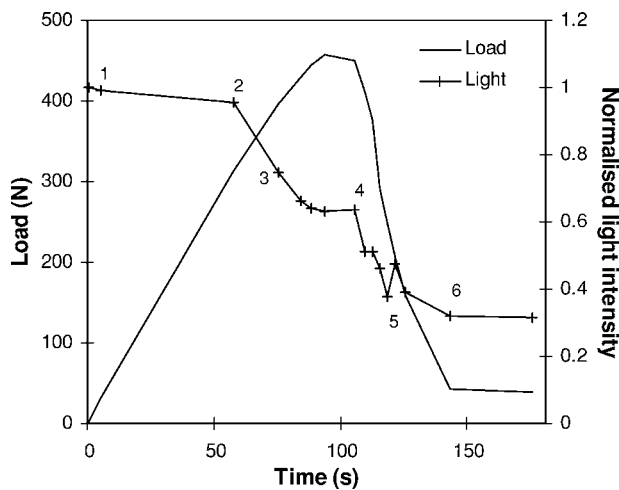


Figure 3 Tensile curve for E-glass fibers and their *in-situ* light transmission variation obtained from the bundle-end images.

determined from the digital images as a function of applied load.

Fig. 2 represents the load-time and normalized transmitted light intensity-time traces for the E-glass waveguide. Here the transmitted light intensity was measured using a photodiode that replaced the CCD-camera. In this experiment involving the uncoated E-glass waveguide, the light transmission intensity decreased gradually up to about 30% of the maximum applied load and further loading resulted in rapid attenuation of the transmitted light. A similar trend was observed when the end of the fiber bundle was imaged and the intensity profile extracted from selected CCD images. The corresponding transmitted light intensity through the E-glass fibers for these images is presented in Fig. 3. Fig. 4 then shows the image selection of a fiber-bundle end during the tensile test. Here, the numbers on this graph correspond to an image in Fig. 4 that has the same number. The general light intensity trend was also observable from the cross-section pictures where the light intensity and the associated areas were reduced. With reference to this test, the photodiode technique gave a more precise light variation and also a facility of use as far as the light intensity was con-

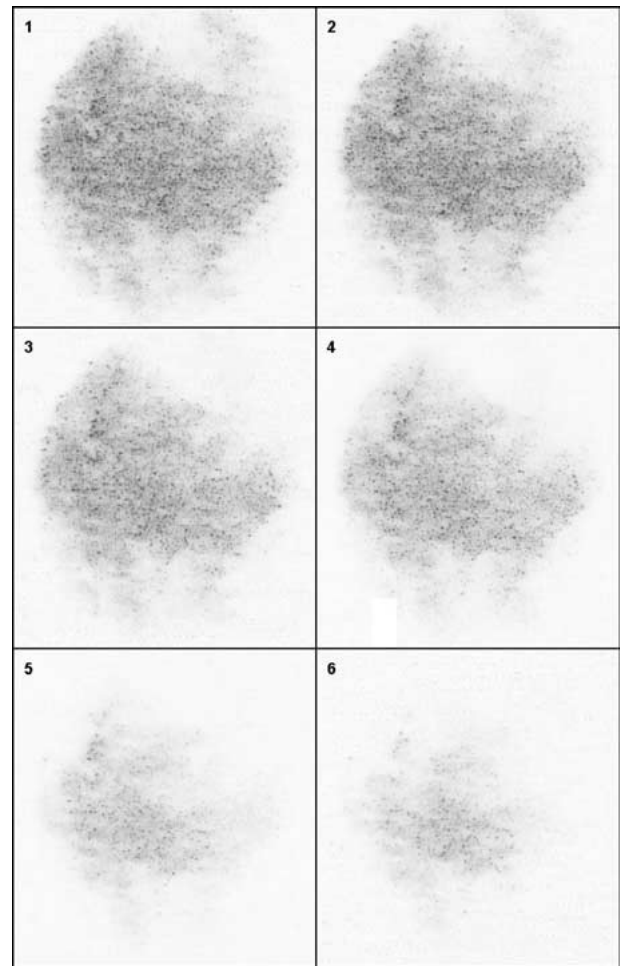


Figure 4 Selection of images of E-glass bundle ends (inverted colors).

cerned. The accuracy of the light attenuation obtained from the images was dependent on the sensitivity of the CCD-camera.

The originality and advantage of the imaging technique could be found in the mapping of the bundle cross-sections. Figs 5 and 6 present 3-D graphs of the sample cross-sections. The graphs were obtained by partitioning the bundle end images into 9×9 arrays, which formed the base of the graphs (x - and y -axes). The z -axis can represent the values of either the light intensity or attenuation in the different arrays. Fig. 5 shows the intensity mapping of the bundle section shown in the images of Fig. 4. From these 3D-graphs, the intensity of the light passing through the bare E-glass fibers was decreasing in amplitude and in area with the increasing applied load. Before reaching the maximum applied load, the light intensity was mainly reduced in the centre of the bundle cross-section as the area of maximum intensity values was reduced without significant reduction of the base surface. This phenomenon was the result of random fiber fracture occurring predominantly in the bundle sections. However, at loads higher than the ultimate load, shrinkage of the transmitting surface resulted in rapid reduction of the light intensity. This was due to predominant fiber fracture at the bundle edge as well as in the cross-section. As a general observation, the light intensity distribution presented a conical shape during the test. This could be explained by the loss of light by evanescence in the

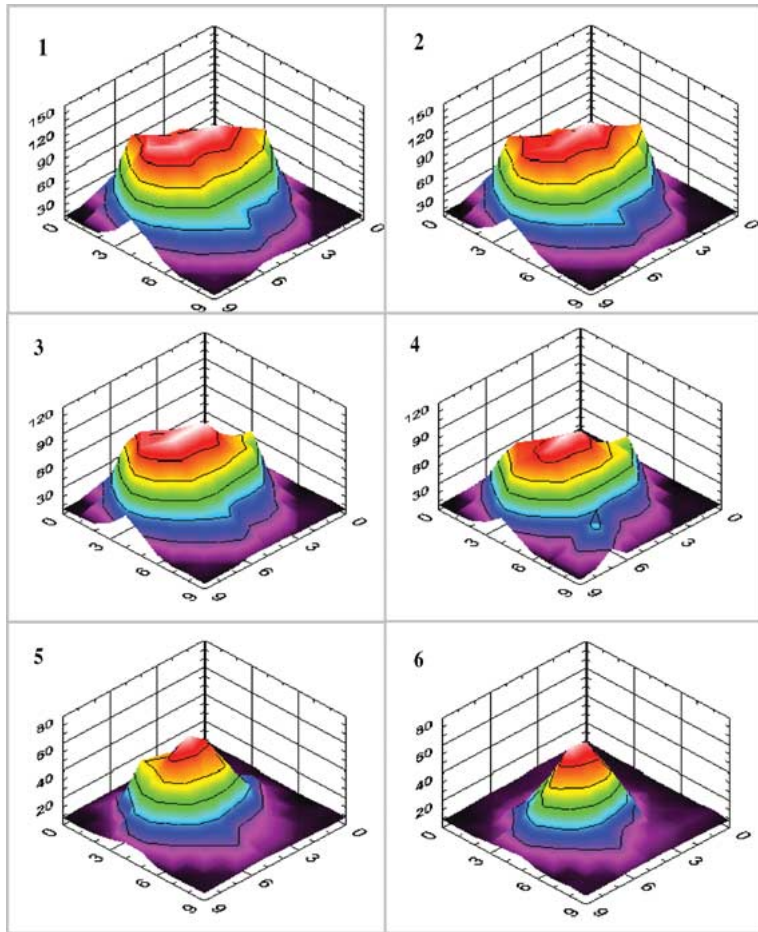


Figure 5 Light-intensity mapping of the E-glass bundle cross-sections shown in the digital images.

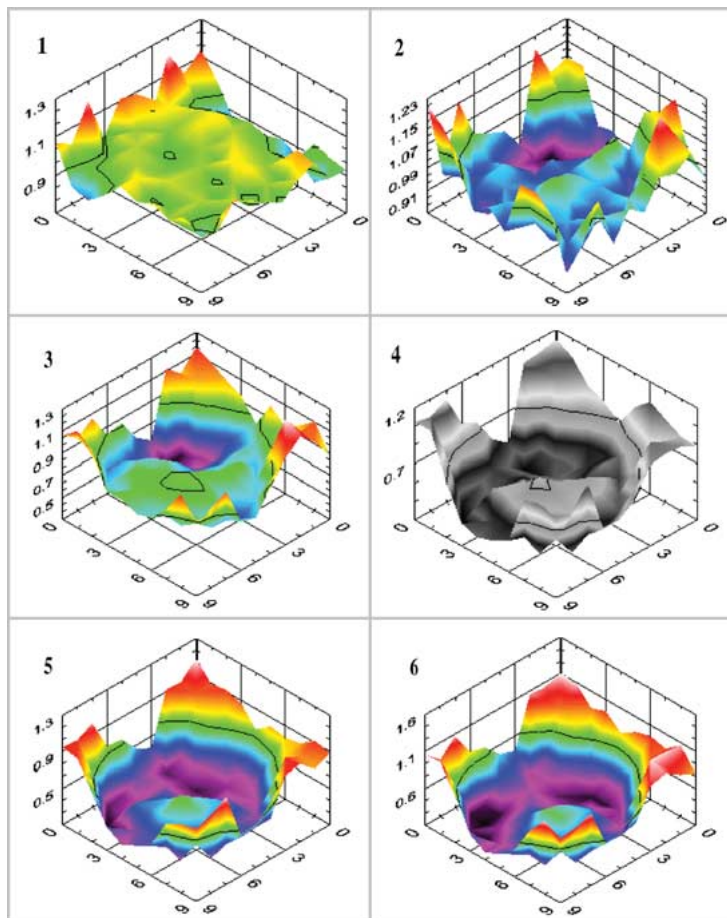


Figure 6 Light-attenuation mapping of the E-glass bundle sections shown in the digital images.

air and in the epoxy-based OG135 resin and also by the light being coupled into neighboring E-glass fibers [11].

Another way of analyzing the bundle images is by mapping the light attenuation across the bundle sections. This mapping of the images is exhibited in Fig. 6 where the z -axis corresponds to the light attenuation. The light attenuation profile presented in these 3D-graphs was determined by considering the attenuation in the initial image (at $t = 0$) to be arbitrary constant to 1 dB. From the graph numbered 1, the light attenuation decreased very slightly in the center of the bundle. This could be the result of the straightening and arrangement of the E-glass fibers at low load. On the other hand, the higher the applied load, the higher the light attenuation. The attenuation increased rapidly in the center of the fiber bundles. This could imply that simultaneously to the shrinkage of the bundle diameter during the test, a high number of fibers in the bundle center was fractured.

It was successfully demonstrated that the cross-sections of E-glass fiber bundles could be imaged using a CCD-camera. From these images, useful information such as light intensity or attenuation either in the whole cross-section or at specific locations could be extracted. The light intensity variation determined from the digital images matched the variation obtained by a photodiode that was in place of the CCD-camera. The mapping of the bundle cross-section demonstrated that fiber fracture occurred at the edge of the bundle as well as at random in the bundle cross-section. In that case, the area of high intensity and the surface of light transmission were reduced, whereas the area of high attenuation was enlarged. By this technique of imaging the end of

E-glass fiber bundles, it would be possible to detect fracture of each individual fiber in a specified area of the bundle cross-section.

Acknowledgments

The authors wish to acknowledge the support of Interglas Technologies (R. Price), RM Consulting (D. Coward and J. Rock) and the EPSRC.

References

1. G. A. SCHOEPPNER and S. ABRATE, *Composites Part A* **31** (2000) 903.
2. M. BASHYAM, *Comp. Eng.* **5** (1995) 735.
3. J. J. LUO, S. C. WOOH and I. M. DANIEL, *J. Compos. Mater.* **29** (1995) 1946.
4. G. N. MORSCHER, *Comp. Sci. Technol.* **59** (1999) 687.
5. J. W. HOLMES and C. CHO, *J. Amer. Ceram. Soc.* **75** (1992) 929.
6. B. HARRIS, in "Engineering Composite Materials" (The Institute of Metals, London, 1986).
7. D. HULL, in "An Introduction of Composite Materials" (Cambridge University Press, 1981).
8. L. R. HWANG, J. W. FERGUS, H. P. CHEN and B. Z. JANG, *Compos. Sci. Technol.* **56** (1996) 1341.
9. F. REBILLAT, A. GUETTE, L. ESPITALIER, C. DEVIEUVRE and R. NASLAIN, *J. Eur. Ceram. Soc.* **18** (1998) 1809.
10. G. KISTER, L. WANG, B. RALPH and G. F. FERNANDO, *Opt. Mater.* **21** (2003) 713.
11. M. GILMORE, in "Fiber Optic Cabling: Theory, Design and Installation Practice" (Newnes, Oxford, 1991).

Received 18 June

and accepted 16 September 2003